18 (2023) 100317

Contents lists available at ScienceDirect

International Journal of Thermofluids

journal homepage: www.sciencedirect.com/journal/international-journal-of-thermofluids

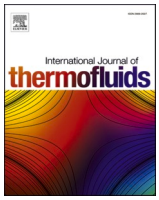

LES analysis on the effects of fire source asymmetry on enhanced wind by fire

Esmaeel Eftekharian [a,*], Maria Rashidi [b], Fatemeh Salehi [c], Bijan Samali [b]

[a] School of Mechanical and Manufacturing Engineering, The University of New South Wales, Sydney, NSW 2052, Australia
[b] Center for Infrastructure Engineering, Western Sydney University, Penrith, NSW 2751, Australia
[c] School of Engineering, Macquarie University, NSW 2113, Australia

ARTICLE INFO

Keywords:
Fire-wind interaction
Wind enhancement
Counter-rotating vortices
Fire source asymmetry

ABSTRACT

Investigation of aerodynamic characteristics of wind enhanced by bushfires is of great significance due to their destructive impacts on buildings located in bushfire-prone areas. Despite the abundance of studies in the fire-wind interaction domain, there have been limited studies concerning the effects of fire on wind aerodynamics. Fire source shape is one of the main factors affecting enhanced wind by fire. This study reports on the effects of fire source asymmetry on aerodynamic changes of wind by fire using a large eddy simulation analysis based on fireFoam solver of OpenFOAM platform. Wind aerodynamic analysis was performed by implementing a module to the solver to extract the corresponding components of fire-induced pressure gradient and acceleration. The results revealed that deviation from fire source symmetry results in asymmetric behaviour of counter-rotating vortices where the maximum cross-sectional wind enhancement occurs. Moreover, the concept of the first-moment area was used to quantify the level of fire source deviation from symmetry and it was shown that the higher first-moment area (about the equivalent symmetry axis) corresponds to a higher deviation from symmetry which delays the realignment of counter-rotating vortices toward the horizontal vortex line.

1. Introduction

The interaction of wind and fire has been the subject of interest for researchers in fire and wind engineering. A comprehensive review of fire-wind interaction behaviour can be found in [1]. The influence of cross-wind on flame characteristics including flame length [2] and flame tilt angle [3,4] was studied. These studies were followed by more comprehensive investigations on flame geometry characteristics for pool fires [5] and jet fires [6] under cross-wind. Comprehensive correlations were developed that predict flame geometry properties for pool and jet fires in presence of cross-wind [5,6].

In contrast to a large number of studies on the effects of wind on flame geometry features, the effects of fire on wind aerodynamic characteristics have only been addressed recently. Eftekharian et al. [7] studied the fundamental mechanisms involved in the influence of fire flame on wind velocity. They revealed that during the interaction of wind with fire, a longitudinal fire-induced pressure gradient is generated in the high-temperature, or low-density region of the fire plume, accelerating the flow and causing enhancement of wind velocity. Subsequent studies were also performed to investigate the effects of various factors contributing to the wind enhancement by fire, including the effects of wind velocity [8,9], fire intensity [10], terrain slope [11–13] and non-dimensional correlations were presented for wind aerodynamic characteristics during fire-wind interaction [10]. In the recent studies on fire-wind enhancement phenomena, the effects of fire source geometry including the type of fire source [14] and fire source aspect ratio [15] on the enhanced wind by fire were studied. The fire source used in all these studies possesses a symmetrical shape. Previous studies mainly focused on the flow induced by a symmetrical fire source which shows the formation of symmetrical counter-rotating vortices downstream of the fire source that correspond to the flow enhancement region [8,16,17]. To the best of the authors' knowledge, there are no studies on the effects of asymmetry of fire source on wind aerodynamic characteristics. Hence, this study aims to address this gap by conducting large eddy simulation (LES) analysis that will enhance understanding of the effects of asymmetrical fire sources on the enhanced wind during fire-wind interaction.

2. Methodology

FireFoam [18] solver of the OpenFOAM platform was used to solve

* Corresponding author.
E-mail address: e.eftekharian@unsw.edu.au (E. Eftekharian).

https://doi.org/10.1016/j.ijft.2023.100317

Available online 23 February 2023

the governing equations, namely continuity, momentum, energy, species, and state equations [8,10]. FireFoam is a transient solver that uses large-eddy simulation and eddy dissipation concepts to treat turbulent structures and combustion modelling.

Momentum equation can be written in the form of flow acceleration as [7,8]:

$$\vec{a} = \frac{D\vec{u}}{Dt} = \frac{-\nabla p}{\rho} + \vec{g} + \frac{\Phi}{\rho} \quad (1)$$

where $\vec{a}$ is the flow acceleration, ρ is the flow density, u is the flow velocity, ∇p is pressure gradient, Φ is the viscous shear stress vector or $(\Phi_i) = \frac{\partial(\sigma_{ji})}{\partial x_j}$ in which σ_{ji} is the component of stress. Eq. (1) demonstrates that the flow acceleration consists of three components, pressure acceleration $\left(\frac{-\nabla p}{\rho}\right)$, gravitational acceleration $(\vec{g})$ and viscous acceleration $\left(\frac{\Phi}{\rho}\right)$. Individual terms in Eq. (1) were implemented to fireFoam solver to perform flow acceleration analysis.

2.1. Geometrical model

A schematic view of the computational domain including a rectangular box with the dimension of 60 m × 18 m × 30 m is shown in Fig. 1. Atmospheric wind velocity profile (power law velocity profile) was used for the domain inlet [8,19]:

$$U_z = U_{ref}\left(\frac{Z}{Z_{ref}}\right)^{\alpha}, \quad (2)$$

where U_{ref} and Z_{ref} indicate the reference mean velocity (3 m/s) and reference height (3 m), respectively. The coefficient α is determined based on the terrain roughness category (here α = 0.16). Different approaches have been used in previous studies to model inflow turbulence for LES simulation in OpenFOAM including the precursor-successor model [20], time-varying turbulent inlet condition [21] and vortex method [8]. In this study, vortex method [22] was used to generate turbulent fluctuations at the domain inlet. To study the effects of fire source asymmetry on the enhanced wind by fire, 6 different fire source shapes including three symmetrical and three asymmetrical sources as shown in Fig. 2 were examined. All the fire source configurations studied have the same fire intensity and fire heat release rates of respectively 6.44 MW/m^2 and 5.22 MW. The no-slip wall boundary condition was prescribed for the domain bottom surface (ground) whereas a slip boundary was used for the domain sides. Pressure outlet and open boundary conditions were applied for the domain outlet and top boundary, respectively. Initial velocity and temperature were set respectively at 0 and 298 K throughout the computational domain. The transient simulation was allowed to progress for the 40 s. This was followed by an additional 20 s for data collection averaging flow variables. This ensures that the wind has traversed the domain length twice before the data collection gets started. We have examined averaging for a longer period (40 s) and no significant difference was observed in the results compared to the case with time-averaging of 20 s.

2.2. Grid sensitivity analysis and validation

Structured grid with total grid number of about 4 million was used for all simulation scenarios. Grid refinement was used such that grid resolution is finer near the fire source with a grid interval size of 0.025 m in the fire source boundary. A grid independence study was performed in our previous works [8,23] using a similar grid structure and simulation settings. It was also shown that for the chosen grid, the ratio between the resolved and total turbulent kinetic energy is 90% in fire plume region which confirms the appropriateness of the selected grid for an LES simulation based on Pope criteria [24].

The applied numerical model was benchmarked with experimental data of buoyant diffusion flame in still condition reported by McCaffrey [25] as well as in wind-fire interaction reported by Hirano and Kinoshita [26]. McCaffrey [25] measured streamwise buoyant diffusion velocity of surface fire with heat release rate of q = 58 kW. Fig. 3(a) shows a schematic view of the generated computational domain to compare the results of the current numerical model with numerical model of Wang et al. [18] and experimental measurement by McCaffrey [25]. Fig. 3(b) reveals that the results of normalised vertical velocity predicted by the current numerical model agree well with previous numerical [18] and experimental [25] data of buoyant diffusion flame. The current numerical model was also validated for wind-fire interaction scenarios in our previous works [7,8], presenting a good agreement between our numerical model with experimental data of Hirano and Kinoshita [26]. Further details of numerical settings and validation for both buoyant diffusion flame and fire-wind interaction can be found in our previous works [7,8].

3. Results and discussion

Fig. 4 shows the cross-sectional time-averaged normalised longitudinal velocity distribution at different distances downstream of the symmetrical fire sources. It can be observed that symmetrical fire sources cause the generation of symmetrical counter-rotating vortices which correspond to the regions with maximum cross-sectional wind enhancement, as observed in previous studies [8,15,16,23]. The region of flow with the greatest wind enhancement is concentrated in both centres of counter-rotating vortices which undergo a gradual expansion with the increase of longitudinal distance from the fire source. This is mainly because the flow longitudinal acceleration, arising from the combined effects of longitudinal fire-induced pressure gradient and low density [7], has the highest intensity in the centres of counter-rotating vortices, as shown in Fig. 5. This region expands with a gradual reduction of flow acceleration and wind enhancement as the longitudinal distance from the fire source increases. At all distances, however, the symmetrical configuration of the fire plume is preserved and causes the

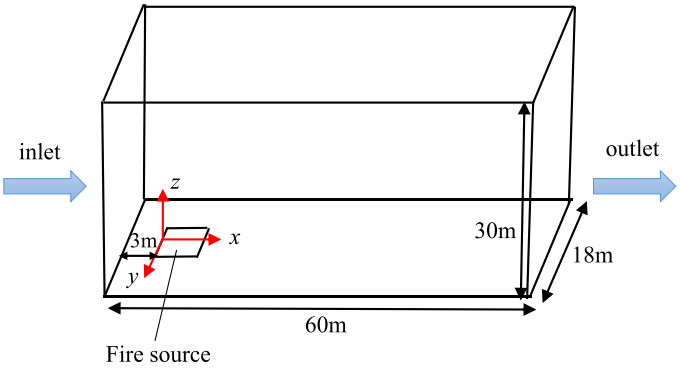

Fig. 1. A schematic view of the computational domain.

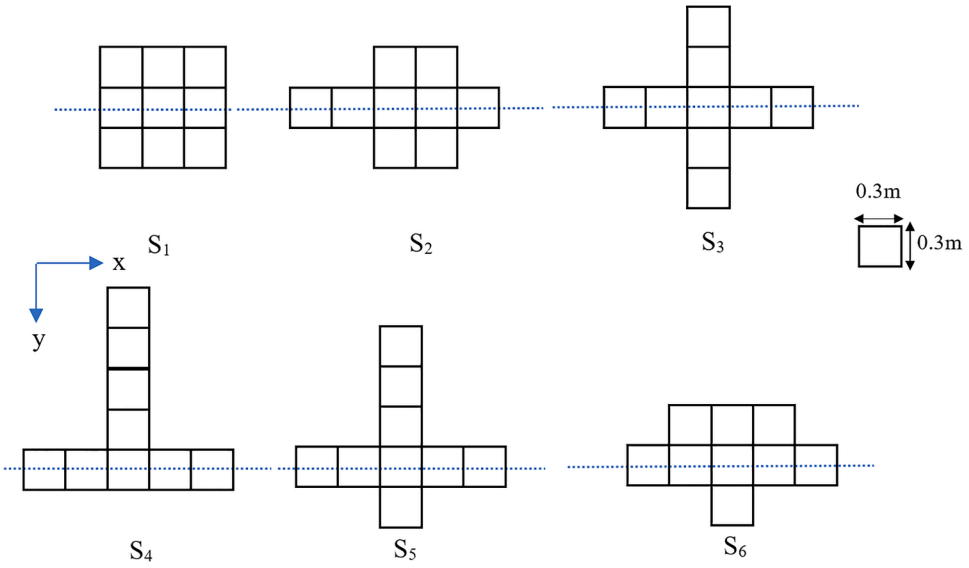

Fig. 2. Different fire sources examined including symmetrical (S_1, S_2, and S_3) and asymmetrical sources (S_4, S_5, S_6). The dotted blue line indicates the equivalent symmetrical axis.

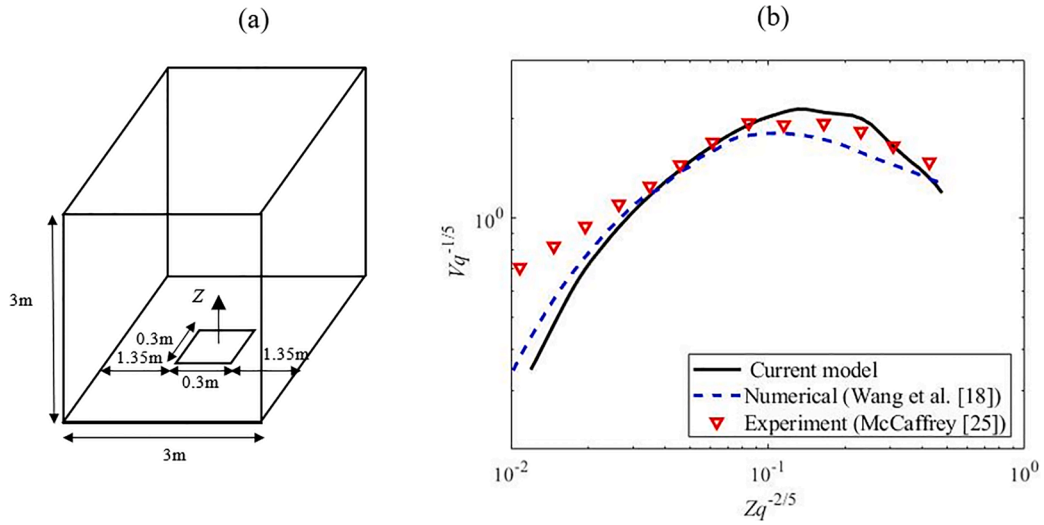

Fig. 3. (a) schematic view of computational domain for validation study (b) comparison of distribution of normalised streamwise velocity (V in Z direction) with previous numerical and experimental data [18,25].

generation of symmetrical counter-rotating vortices and the corresponding equal wind acceleration and enhancement at the centre of each vortex. This symmetrical behaviour of wind enhancement for symmetrical fire source geometry was also observed in previous studies [8,15]. Fig. 4 also reveals that the more concentrated the source is, the lower the maximum wind enhancement. In other words, for the scenarios with the same fire intensity, fire heat release rate, and free-stream wind velocity, the fire sources with a higher spatial expansion, induce a stronger enhanced wind. This is primarily caused by a lower level of fire-induced wind acceleration in concentrated sources, causing a weaker wind enhancement for S_1 followed by S_2 and S_3, as observed in Fig. 4.

Fig. 6, however, shows how deviation from fire source symmetry affects wind enhancement behaviour downstream of the fire source. Fig. 6 reveals that deviation from fire source symmetry disturbs the counter-rotating vortex balance observed for symmetrical cases in Fig. 4. This behaviour is because of an imbalance in fire-induced acceleration at the location of counter-rotating vortices induced by asymmetrical fire sources, as observed in Fig. 7. Taking S_3 in Fig. 2. as the basis symmetry source, S_4 has the highest deviation from symmetry followed by S_5 and S_6. Here, we quantify deviation from symmetry by calculating the first-moment area about the equivalent symmetrical axis (plotted as blue dotted lines in Fig. 2. (S_3)). First-moment area for S_4, S_5, and S_6 scenarios is therefore $(Q_{xx})_{S_4} = 0.27$, $(Q_{xx})_{S_5} = 0.135$, $(Q_{xx})_{S_6} = 0.054$, respectively. Evidently, this value is zero for the basis symmetrical source (S_3). Sub figures in Fig. 6, depict that deviation from a symmetrical fire source geometry results in asymmetrical behaviour of counter-rotating vortices as such one of the vortices' locations is shifted to a higher elevation. To better explain the impact of fire source asymmetry on wind enhancement, the vortex line which is referred to as the line connecting the locations of maximum cross-sectional local wind enhancement at each vortex is plotted in Figs. 4 and 6. It can be observed that the vortex line is horizontal for symmetrical fire sources while it turns into a slope line in asymmetrical fire source scenarios. A comparison of different columns in Fig. 6 demonstrates that fire sources with a higher first-moment area about the equivalent symmetry line exhibit a higher vortex line slope. Fig. 6 also reveals that for all asymmetrical fire source scenarios, the

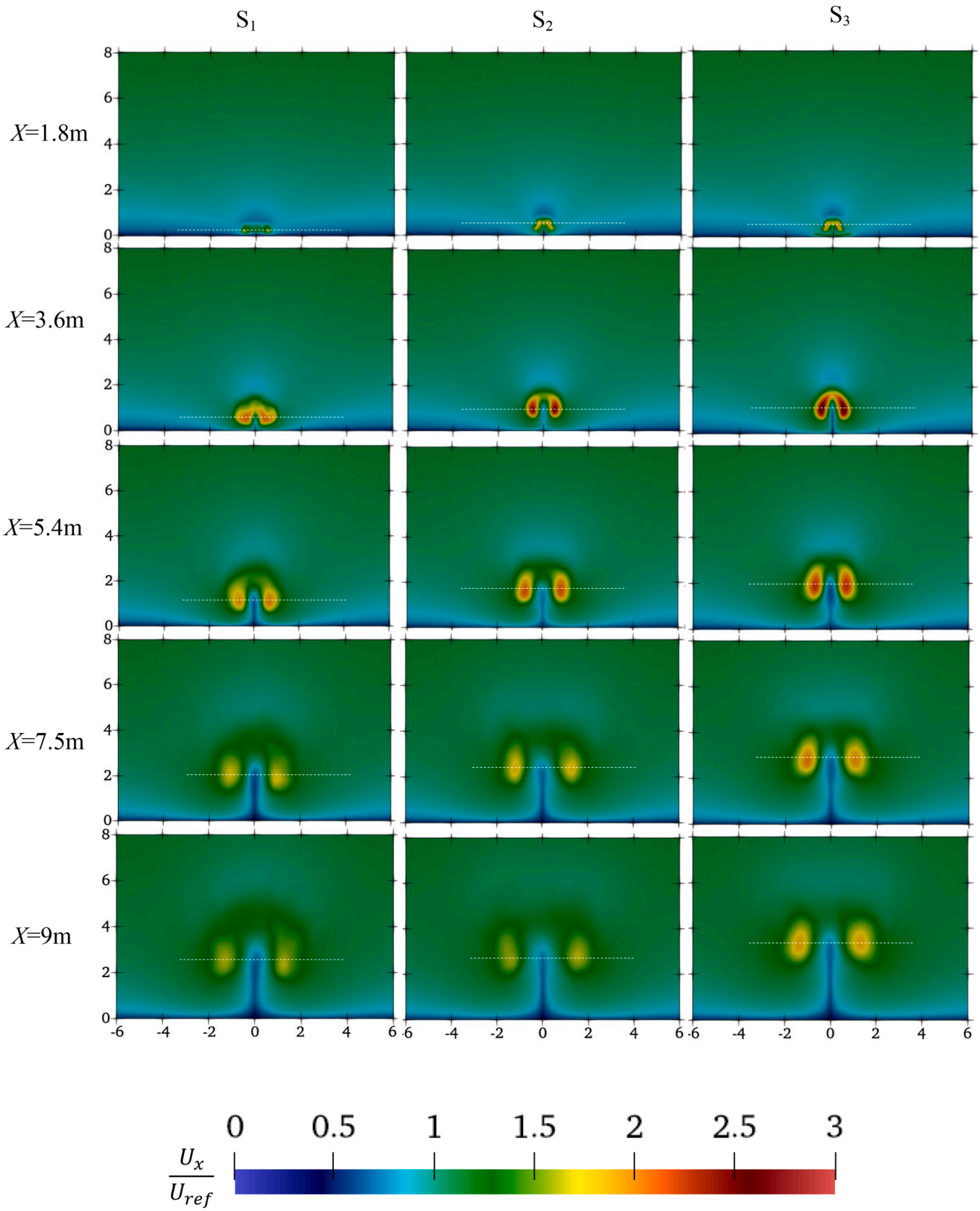

Fig. 4. Cross-sectional distribution of time-averaged normalised longitudinal flow velocity at different distances downstream of the fire source for symmetrical fire sources (S_1, S_2, and S_3). (The horizontal and vertical axis in each sub-figure corresponds to Y (m) and Z (m) directions, respectively).

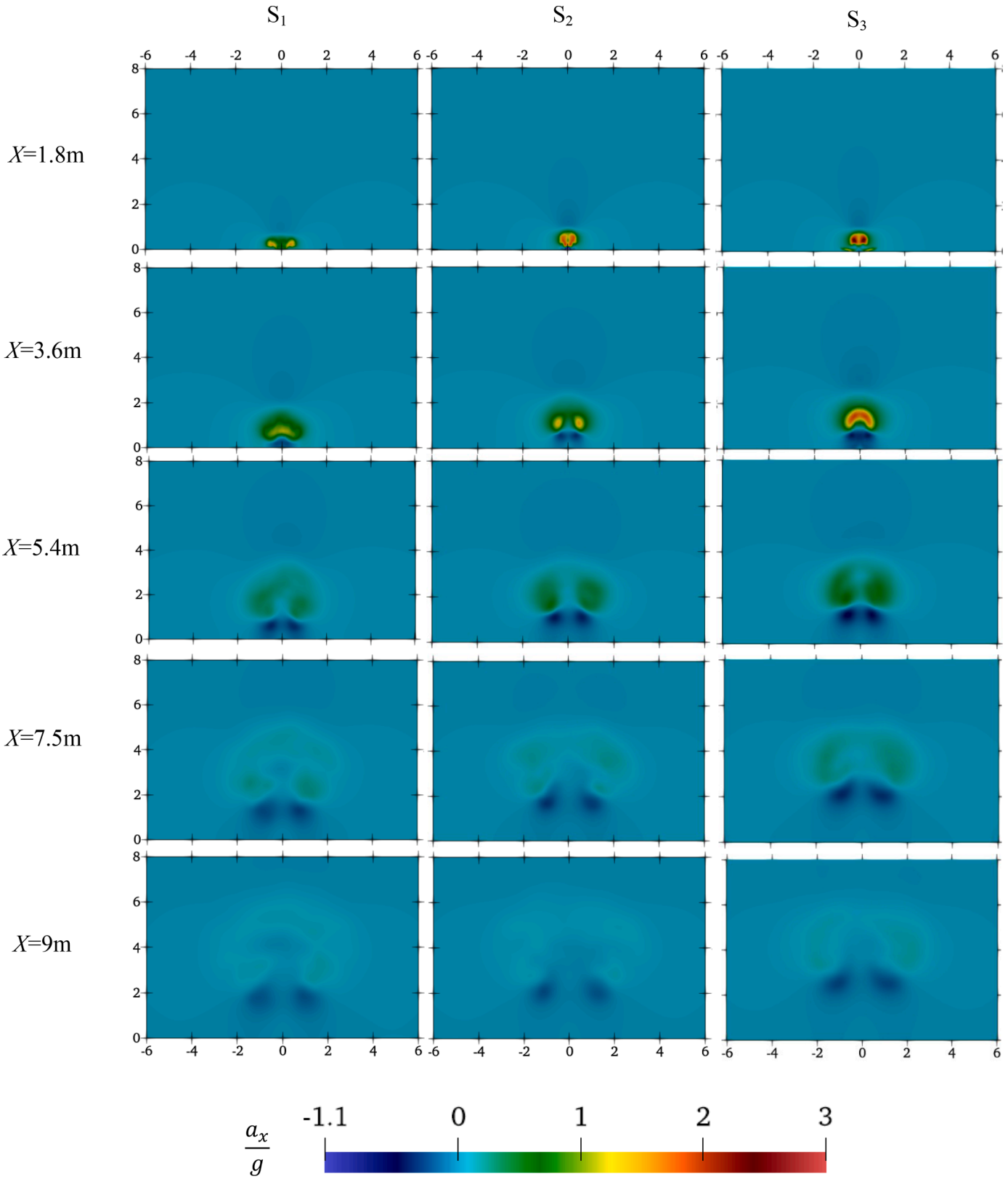

Fig. 5. Cross-sectional distribution of time-averaged normalised longitudinal flow acceleration at different distances downstream of the fire source for symmetrical fire sources (S_1, S_2, and S_3). (The horizontal and vertical axis in each sub-figure corresponds to Y (m) and Z (m) directions, respectively).

vortex line slope first increases immediately downstream of the fire sources, reaching a maximum value and undergoing a gradual reduction further downstream of the fire source. The vortex line is finally inclined to the horizontal line at a sufficient longitudinal distance downstream of the fire source. This inclination towards a horizontal vortex line is delayed for scenarios with a higher first-moment area about the equivalent symmetry axis.

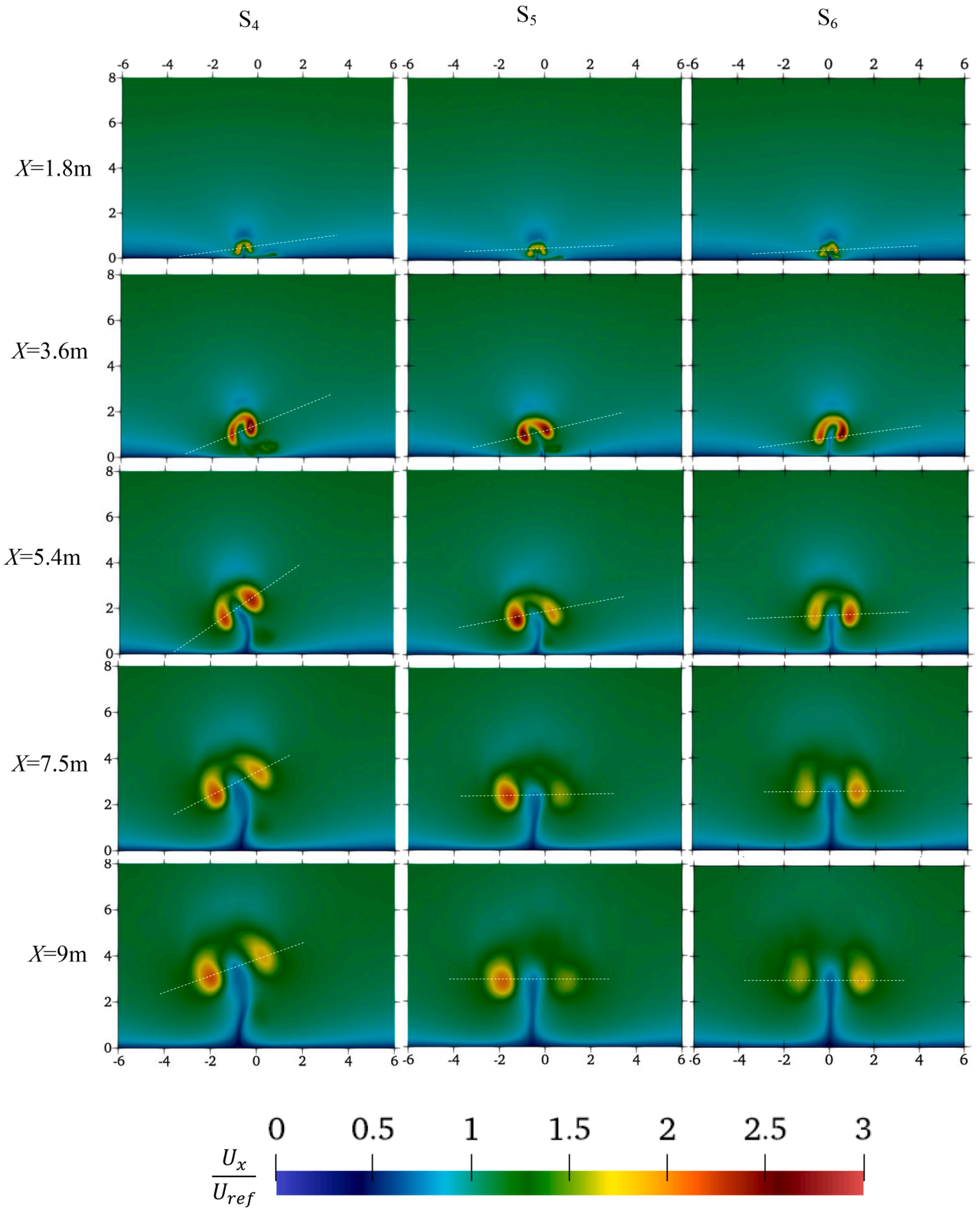

Fig. 6. Cross-sectional distribution of time-averaged normalised longitudinal flow velocity at different distances downstream of the fire source for asymmetrical fire sources (S_4, S_5, and S_6). (The horizontal and vertical axis in each sub-figure corresponds to Y (m) and Z (m) directions, respectively).

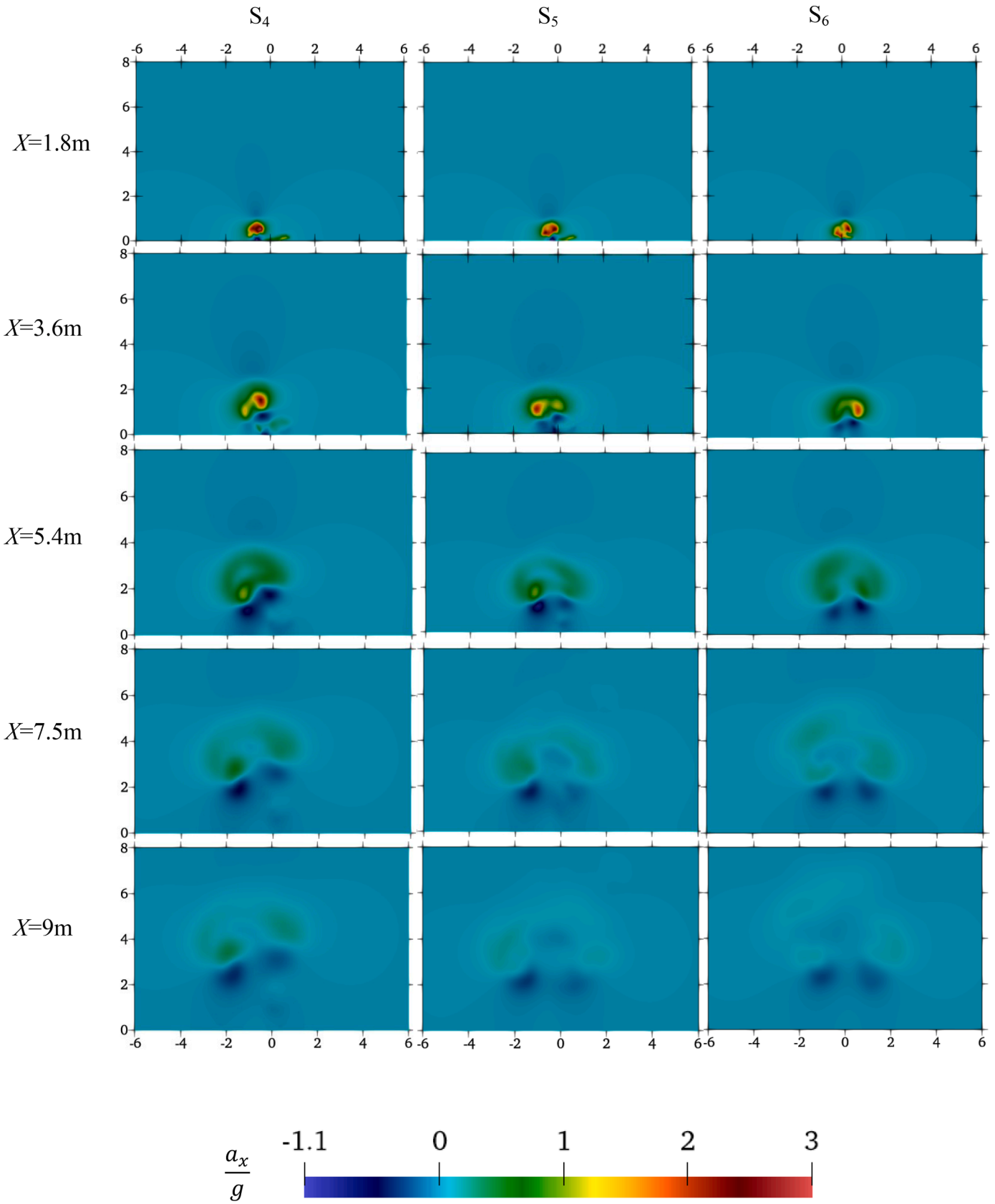

Fig. 7. Cross-sectional distribution of time-averaged normalised longitudinal flow acceleration at different distances downstream of the fire source for asymmetrical fire sources (S_4, S_5, and S_6). (The horizontal and vertical axis in each sub-figure corresponds to Y (m) and Z (m) directions, respectively).

4. Conclusion

Large eddy simulation analysis was performed to investigate the effects of fire source asymmetry on the enhanced wind by fire. Six different fire sources including three symmetrical and three asymmetrical sources were examined under identical fire intensity and fire heat release rate conditions. Fire-induced acceleration analysis was performed to explain the extent to which fire source asymmetry affects enhanced wind by fire. Deviation of wind enhancement characteristics from symmetry in asymmetrical fire source scenarios was quantified using the concept of the first-moment area about the equivalent symmetry line and it was shown that the higher the first-moment of area, the higher the deviation from symmetry. An asymmetrical fire source was shown to trigger an imbalance in the locations of counter-rotating vortices and wind enhancement region immediately downstream of the fire source, causing one of the vortices and the corresponding wind enhancement region to stand at a higher elevation. The results also reveal that the imbalance of counter-rotating vortices and wind enhancement associated with an asymmetrical fire source is intensified as the first-moment area of the fire source increases.

Declaration of Competing Interest

The authors declare that they have no known competing financial interests or personal relationships that could have appeared to influence the work reported in this paper.

Data availability

Data will be made available on request.

References

[1] L. Hu, A review of physics and correlations of pool fire behaviour in wind and future challenges, Fire Saf. J. 91 (Supplement C) (2017) 41–55.
[2] L. Hu, L. Wu, S. Liu, Flame length elongation behavior of medium hydrocarbon pool fires in cross air flow, Fuel 111 (2013) 613–620.
[3] Y. Oka, H. Kurioka, H. Satoh, O. Sugawa, Modelling of unconfined flame tilt in cross-winds, Fire Saf. Sci. 6 (2000) 1101–1112.
[4] L. Hu, S. Liu, J.L. de Ris, L. Wu, A new mathematical quantification of wind-blown flame tilt angle of hydrocarbon pool fires with a new global correlation model, Fuel 106 (2013) 730–736.
[5] Y. Lin, M.A. Delichatsios, X. Zhang, L. Hu, Experimental study and physical analysis of flame geometry in pool fires under relatively strong cross flows, Combust. Flame 205 (2019) 422–433.
[6] H. Lu, M.A. Delichatsios, X. Li, S. Liu, J. Lv, L. Hu, Flame geometry of downward buoyant turbulent jet fires under cross flows: experiments, dimensional analysis and an integral model, Proc. Combust. Inst. 38 (3) (2021) 4917–4925.
[7] E. Eftekharian, Y. He, K.C.S. Kwok, R.H. Ong, J. Yuan, Investigation of fire-driven cross-wind velocity enhancement, Int. J. Therm. Sci. 141 (2019) 84–95.
[8] E. Eftekharian, M. Ghodrat, Y. He, R.H. Ong, K.C.S. Kwok, M. Zhao, Numerical analysis of wind velocity effects on fire-wind enhancement, Int. J. Heat Fluid Flow 80 (2019), 108471.
[9] E. Eftekharian, M. Ghodrat, R. Ong, Y. He, K. Kwok, CFD investigation of cross-flow effects on fire-wind enhancement, in: Australasian Fluid Mechanics Conference, 2018. Adelaide, Australia.
[10] E. Eftekharian, M. Ghodrat, Y. He, R.H. Ong, K.C.S. Kwok, M. Zhao, Correlations for fire-wind enhancement flow characteristics based on LES simulations, Int. J. Heat Fluid Flow 82 (2020), 108558.
[11] E. Eftekharian, M. Ghodrat, Y. He, R.H. Ong, K.C.S. Kwok, M. Zhao, B. Samali, Investigation of terrain slope effects on wind enhancement by a line source fire, Case Stud. Therm. Eng. 14 (2019), 100467.
[12] E. Eftekharian, M. Rashidi, M. Ghodrat, Y. He, K.C.S. Kwok, LES simulation of terrain slope effects on wind enhancement by a point source fire, Case Stud. Therm. Eng. 18 (2020), 100588.
[13] E. Eftekharian, M. Ghodrat, Y. He, R.H. Ong, K.C. Kwok, B. Samali, Numerical simulation of the effect of terrain slope on fire-wind enhancement, in: ACMSM25, 2020, pp. 1087–1096. Springer.
[14] E. Eftekharian, M. Ghodrat, Y. He, R.H. Ong, K.C.S. Kwok, M. Zhao, Numerical analysis of the effect of fire source configuration on fire-wind enhancement, Heat Transf. Eng. 42 (2021) 41–60.
[15] E. Eftekharian, F. Salehi, Y. He, K.C.S. Kwok, LES analysis of fire source aspect ratio effects on fire-wind enhancement, Int. J. Heat Fluid Flow 89 (2021), 108803.
[16] B. Li, L. Ding, A. Simeoni, J. Ji, H. Wan, L. Yu, Numerical investigation of the flow characteristics around two tandem propane fires in a windy environment, Fuel 286 (2021), 119344.
[17] P. Cunningham, S.L. Goodrick, M.Y. Hussaini, R.R. Linn, Coherent vortical structures in numerical simulations of buoyant plumes from wildland fires, Int. J. Wildland Fire 14 (1) (2005) 61–75.
[18] Y. Wang, P. Chatterjee, J.L. de Ris, Large eddy simulation of fire plumes, Proc. Combust. Inst. 33 (2) (2011) 2473–2480.
[19] T.-.K. Liu, D. Jamshideasli, B. Ramezanpour, W. Ye, Y. Zeng, O.A. Zargar, S.C. Hu, J.M. Khodadadi, G. Leggett, Control of flow, thermal and pollutant concentration fields by entrainer air streams to improve fresh air quality intake into a semiconductor manufacture/processing plant, Int. J. Thermofluids 16 (2022), 100211.
[20] R.H. Ong, L. Patruno, Y. He, E. Efthekarian, Y. Zhao, G. Hu, K.C.S. Kwok, Large-eddy simulation of wind-driven flame in the atmospheric boundary layer, Int. J. Therm. Sci. 171 (2022), 107032.
[21] S.Z. Dizjeh, J. Brinkerhoff, Numerical investigations of turbulent heat transfer enhancement in circular tubes via modified internal profiles, Int. J. Thermofluids 16 (2022), 100237.
[22] F. Mathey, D. Cokljat, J.P. Bertoglio, E. Sergent, Assessment of the vortex method for large eddy simulation inlet conditions, Prog. Comput. Fluid Dyn. 6 (1–3) (2006) 58–67.
[23] E. Eftekharian, F. Salehi, Y. He, K.C.S. Kwok, LES analysis on the effects of baroclinic generation of vorticity on fire-wind enhancement, Int. J. Therm. Sci. 162 (2021), 106775.
[24] S.B. Pope, S.B. Pope, Turbulent Flows, Cambridge University Press, 2000.
[25] McCaffrey, B.J., C.f.F. Research, and U.S.N.B.o. Standards, Purely buoyant diffusion flames: some experimental results. 1979.
[26] T. Hirano, M. Kinoshita, Gas velocity and temperature profiles of a diffusion flame stabilized in the stream over liquid fuel, Symp. (Int.) Combust. 15 (1) (1975) 379–387.